

Adaptive Artificial Time-Delay Control with Barrier Lyapunov Constraints for Euler–Lagrange Robots

Saksham Gupta¹, Rishabh Dev Yadav², Sarthak Mishra¹, Amitabh Sharma¹, Sourish Ganguly¹, Wei Pan³, Spandan Roy¹ and Simone Baldi⁴

Abstract—This paper addresses the challenge of simultaneously compensating for state-dependent uncertainties and enforcing time-varying state constraints in Euler–Lagrange systems—a common requirement in robotics yet underserved by existing control designs. A novel adaptive control framework is developed that combines an artificial time delay based uncertainty estimation (aka time delay estimation, TDE) strategy with a barrier Lyapunov function to enforce constraint-aware control design. Specifically, a state-dependent upper bound on the TDE approximation error is analytically formulated, and an adaptive law is constructed to estimate its parameters online, enabling real-time state-dependent uncertainty compensation without relying on prior model knowledge. To ensure constraint compliance, the barrier Lyapunov function-based controller enforces time-varying bounds on both position and velocity. The resulting architecture is provably stable via Lyapunov analysis. Experimental results on a five degrees-of-freedom robotic manipulator validate the framework’s capability over the state-of-the-art in maintaining strict adherence to safety-critical constraints under dynamic uncertainties.

I. INTRODUCTION

Robotic systems are increasingly deployed in dynamic and uncertain environments, where safety, stability, and high performance are essential. Achieving reliable operation in such settings is particularly challenging due to the nonlinear Euler–Lagrange (EL) dynamics of the robots, and due to the effects of uncertain parameters and unmodeled terms. In these contexts, control strategies

The work is partly supported by the UASAT project sponsored by MeITY, India. The work is partly supported by the UASAT project sponsored by MeITY, India. The work is partly supported by the UASAT project sponsored by MeITY, India.

¹The authors are with Robotics Research Center, International Institute of Information Technology Hyderabad, India. emails: {sakshammgupta, sourishganguly96}@gmail.com, {sarthak.mishra, amitabh.sharma}@research.iiit.ac.in, spandan.roy@iiit.ac.in

²R. D. Yadav is with Department of Computer Science, University of Manchester, UK. email: rishabh.yadav@postgrad.manchester.ac.uk

³W. Pan is with Autonomous Systems and Automatic Control in School of Engineering, Newcastle University, UK. email: wei.pan2@newcastle.ac.uk

⁴S. Baldi is with Self-Organizing Mobility Lab, School of Mathematics, Southeast University, Nanjing 210096, China, email: simonebaldi@seu.edu.cn

must operate reliably despite incomplete system knowledge, while enforcing state constraints to ensure task feasibility and safety. The simultaneous need for uncertainty compensation and real-time constraint satisfaction defines a central challenge in robotics.

A. Related Works and Motivation

Artificial time delay control (also known as time-delay estimation or TDE-based control) was introduced to reduce reliance on system models by approximating unknown dynamics using delayed state/input measurements [1], [2]. Its simplicity and low computational cost have led to widespread adoption in robotics [3]–[10]. However, most TDE-based methods [3]–[10] assume an a priori known bound on the approximation error—an assumption that limits robustness to fast-varying or state-dependent uncertainties. To overcome this limitation, adaptive TDE control frameworks have been proposed by [11]–[13], wherein a structured state-dependent upper bound on the TDE error is analytically formulated and its parameters are updated online via adaptive laws. However, these methods do not incorporate mechanisms for enforcing state constraints, making them unsuitable for safety-critical applications where real-time enforcement of position and velocity limits is essential.

In many practical applications, ensuring that system states remain within prescribed bounds is as critical as achieving tracking accuracy. Robotic arms operating near humans, aerial vehicles navigating constrained spaces, or manipulators handling delicate payloads, all demand strict enforcement of position and velocity limits for safety and reliability. While Model Predictive Control (MPC) can tackle such constraints, it requires accurate model and imposes high computational overhead — making it unsuitable for many embedded robotic systems [14]–[17]. Barrier Lyapunov Functions (BLFs), by contrast, encode constraints directly into the control design, enabling real-time enforcement without online optimization [18]–[22].

Although early BLF-based control strategies required precise knowledge of system dynamics, more recent designs have relaxed this dependency by incorporating robust [23]–[25] or adaptive [26]–[31] mechanisms. However, the majority of these methods enforce position-

only (i.e., partial state) constraints, which significantly reduce flexibility (cf. [18], [19], [24], [25], [27]). To address this, time-varying BLF formulations have been developed ([21], [32]–[35]), offering improved constraint scheduling. Nevertheless, many of these approaches still rely on accurate model information (cf. [21], [32], [33]) or assume a priori bounded uncertainty (cf. [34], [35]). This is a critical limitation for EL systems, where uncertainty is inherently state-dependent and cannot be bounded in advance. As shown in [36], relying on a priori bounded uncertainty in adaptive control design can even compromise stability.

B. Contribution

These limitations motivate the development of an adaptive-robust control framework that explicitly addresses both constraint enforcement and uncertainty adaptation in a unified manner. This framework simultaneously addresses state-dependent uncertainty and time-varying position and velocity constraints—two critical but often separately treated challenges in nonlinear control. The key contributions are:

- **State-dependent uncertainty adaptation:** A novel TDE formulation is derived with an explicit, structured upper bound on the approximation error. The bound’s parameters are adapted online, enabling compensation of unknown, state-dependent terms.
- **Time-varying constraint enforcement:** A BLF-based control strategy is developed to rigorously enforce time-varying position and velocity constraints, accommodating initial errors and transients.
- **Cohesive design:** The controller tightly couples adaptive uncertainty estimation and constraint satisfaction in a provably stable architecture. Stability and constraint compliance are formally established through Lyapunov analysis.

To the best of our knowledge, this is the first framework to couple Adaptive TDE with BLF-based constraint enforcement for nonlinear EL-based robotic systems. The approach is validated on a 5-degrees-of-freedom (DoF) robotic manipulator, outperforming the state of the art.

The rest of the paper is organised as follows: Section II describes the EL robotics dynamics and the control problem; Section III details the proposed control framework, while corresponding stability analysis is provided in Section IV; comparative experimental results are in Section V, while Section VI provides concluding remarks.

The following notations are used in the paper: $(\bullet)_L$ denotes that $(\bullet)(t)$ is delayed by L , i.e., $(\bullet)(t - L)$; $\lambda_{\min}(\bullet)$, $\lambda_{\max}(\bullet)$, $\|\bullet\|$, $|\bullet|$ denote minimum and maximum eigenvalue, 2-norm and absolute value of

• respectively; $I_n \in \mathbb{R}^{n \times n}$ denotes Identity matrix; $\text{diag}\{\cdot, \dots, \cdot\}$ denotes a diagonal matrix with diagonal elements $\{\cdot, \dots, \cdot\}$; \exp denotes exponential function; the saturation function $\text{sat}(s, \varpi) = (s/\|s\|)$ if $\|s\| \geq \varpi$ and $\text{sat}(s, \varpi) = (s/\varpi)$ if $\|s\| < \varpi$ with $\varpi \in \mathbb{R}^+$.

II. SYSTEM DYNAMICS AND PROBLEM FORMULATION

Let us consider the following class of robots modeled via Euler-Lagrange (EL) dynamics [3]–[10]:

$$M(q(t))\ddot{q}(t) + H(q(t), \dot{q}(t), t) = \tau(t), \quad (1)$$

where $q, \dot{q} \in \mathbb{R}^n$ are the system states (position and velocity), $\tau \in \mathbb{R}^n$ is the generalized control input, $M \in \mathbb{R}^{n \times n}$ is the mass/inertia matrix and $H \in \mathbb{R}^n$ represents the combined effects of dynamic forces (e.g., Coriolis, dissipative, restoring, external disturbances etc.).

The following system property holds from standard EL mechanics [37]:

Property 1: The matrix $M(q)$ is uniformly positive definite for all q , i.e., $\exists \psi_1, \psi_2 \in \mathbb{R}^+$ such that

$$\psi_1 I \leq M(q) \leq \psi_2 I \Rightarrow (1/\psi_2)I \leq M^{-1}(q) \leq (1/\psi_1)I. \quad (2)$$

Let us introduce the amount of uncertainty in system as follows:

Remark 1 (Uncertainty): The precise knowledge of M is not available, only its upper bound (ψ_2) is known. Whereas, H is unknown for control design.

Introducing a constant diagonal matrix \bar{M} , the dynamics (1) can be compactly written as

$$\bar{M}\ddot{q} + N(q, \dot{q}, \ddot{q}) = \tau, \quad (3)$$

$$\text{with } N(q, \dot{q}, \ddot{q}) = [M(q) - \bar{M}]\ddot{q} + H(q, \dot{q}) \quad (4)$$

and the selection of \bar{M} is discussed later (cf. Remark 3). The desired trajectories $q^d(t)$ and their time-derivatives $\dot{q}^d(t)$, $\ddot{q}^d(t)$ are designed to be smooth and bounded. The signals $(q(t), \dot{q}(t), \ddot{q}(t))$ are available for control design.

Control Objective: Let the position and velocity tracking errors (e, \dot{e}) be defined as

$$e = q - q^d; \quad \dot{e} = \dot{q} - \dot{q}^d. \quad (5a)$$

Let us decompose $e = [e_1 \ e_2 \ \dots \ e_n]^T$, $\dot{e} = [\dot{e}_1 \ \dot{e}_2 \ \dots \ \dot{e}_n]^T$, where e_i and \dot{e}_i the tracking errors for the i^{th} degree-of-freedom, $i = 1, 2, \dots, n$. Since we are interested in tracking control, the problem of imposing constraints on states q, \dot{q} can be equivalently considered to be the problem of imposing constraints on tracking errors e, \dot{e} around desired trajectories (cf. (5)). Accordingly, we define constraint functions

$$k_{pi}(t) = (k_{0pi} - k_{sspi}) \exp^{-\alpha_p t} + k_{sspi}, k_{0pi} > e_i(0) \quad (6a)$$

$$k_{vi}(t) = (k_{0vi} - k_{ssvi}) \exp^{-\alpha_v t} + k_{ssvi}, k_{0vi} > \dot{e}_i(0) \quad (6b)$$

where $\alpha_p, \alpha_v \in \mathbb{R}^+$ are scalars; (k_{0pi}, k_{0vi}) and (k_{sspi}, k_{ssvi}) are the initial and steady-state values of the

respective constraints. Our control objective is to keep the tracking errors within the constraints as $|e_i(t)| < k_{pi}(t)$, $|\dot{e}_i(t)| < k_{vi}(t)$ for all time $t \geq 0$. In the following, we discuss the design of the constraint functions (6).

Remark 2 (Design of constraint function): To have a well-posed initial setting, initial tracking errors should satisfy $|e_i(0)| < k_{pi}(0)$, $|\dot{e}_i(0)| < k_{vi}(0)$, as standard in the literature [18]–[21], [23]–[35]. This can be used to define (k_{0pi}, k_{0vi}) ; whereas, (k_{sspi}, k_{ssvi}) can be selected based on user-defined steady-state bounds. Further, the parameters $(\alpha_{pi}, \alpha_{vi})$ determine the convergence rate, which can be as per application requirements.

III. PROPOSED ADAPTIVE CONTROL SOLUTION

Variable dependency will be removed subsequently for brevity whenever it is obvious. The control input τ is designed as

$$\tau = \bar{M}u + \hat{N}(q, \dot{q}, \ddot{q}), \quad (7a)$$

$$\text{with } u = u_0 - \Delta u, \quad (7b)$$

$$\hat{N}(q, \dot{q}, \ddot{q}) \cong N(q_L, \dot{q}_L, \ddot{q}_L) = \tau_L - \bar{M}\ddot{q}_L, \quad (7c)$$

$$u_0 = \ddot{q}^d - D_D \dot{e} - D_P e, \quad (7d)$$

$$D_P = \text{diag} \left\{ \frac{1}{k_{p1}^2 - e_1^2}, \dots, \frac{1}{k_{pn}^2 - e_n^2} \right\}, \quad (7e)$$

$$D_D = \text{diag} \left\{ \frac{1}{k_{v1}^2 - \dot{e}_1^2}, \dots, \frac{1}{k_{vn}^2 - \dot{e}_n^2} \right\}, \quad (7f)$$

and Δu is the adaptive control term to be designed later; \hat{N} is the estimate of the uncertainty function N derived from the past state/input data; $L > 0$ is a small time delay introduced to collect the past data and its choice is discussed later (cf. Remark 4). *This estimation process via artificial/intentional injection of delay is conventionally called time-delay estimation (TDE).*

Substituting (7a), (7b) and (7d) into (3) gives the following error dynamics:

$$\ddot{e} = -D_D \dot{e} - D_P e + \sigma - \Delta u, \quad (8)$$

where $\sigma = \bar{M}^{-1}(N - \hat{N})$ is the *estimation error* stemming from TDE process (7c) and it is termed as the *TDE error*. The adaptive control term Δu is designed based on the structure of the upper bound of TDE error $\|\sigma\|$ derived subsequently.

A. Upper bound structure of $\|\sigma\|$

From (1) and (8), the following relations can be achieved:

$$\hat{N} = N_L = [M(q_L) - \bar{M}]\ddot{q}_L + H_L, \quad (9)$$

$$\sigma = \ddot{q} - u. \quad (10)$$

Using (9), the control input τ in (7a) can be rewritten as

$$\tau = \bar{M}u + [M(q_L) - \bar{M}]\ddot{q}_L + H_L. \quad (11)$$

Multiplying both sides of (10) with M and using (1) and (11)

$$\begin{aligned} M\sigma &= \tau - H - Mu, \\ &= \bar{M}u + [M(q_L) - \bar{M}]\ddot{q}_L + H_L - H - Mu. \end{aligned} \quad (12)$$

Defining $D \triangleq [D_P \ D_D]$, $\xi \triangleq [e^T \ \dot{e}^T]^T$ and using (8) we have

$$\ddot{q}_L = \ddot{q}_L^d - D\xi_L + \sigma_L - \Delta u_L. \quad (13)$$

Substituting (13) into (12), and after re-arrangement yields

$$\begin{aligned} \sigma &= \underbrace{M^{-1}\bar{M}(\Delta u_L - \Delta u)}_{x_1} + \underbrace{M^{-1}(M\Delta u - M_L\Delta u_L)}_{x_2} \\ &+ \underbrace{M^{-1}\{(\bar{M} - M)\ddot{q}^d + (M_L - \bar{M})\ddot{q}_L^d + H_L - H\}}_{x_3} \\ &+ \underbrace{(I - M^{-1}\bar{M})D\xi}_{x_4} + \underbrace{M^{-1}(\bar{M} - M_L)D\xi_L}_{x_5} \\ &+ \underbrace{M^{-1}(M_L - \bar{M})\sigma_L}_{x_6}. \end{aligned} \quad (14)$$

Both M and M^{-1} are bounded from system property (2). Using the relation $(\cdot)_L = (\cdot)(t) - \int_{-L}^0 \frac{d}{d\theta}(\cdot)(t+\theta)d\theta$ and the fact that integration of any continuous function over a finite interval (here $-L$ to 0) is always finite [38], the following conditions hold for unknown constants δ_i , $i = 1, \dots, 6$:

$$\|\chi_1\| = \|-M^{-1}\bar{M} \int_{-L}^0 \frac{d}{d\theta} \Delta u(t+\theta)d\theta\| \leq \delta_1 \quad (15a)$$

$$\|\chi_2\| = \|M^{-1} \int_{-L}^0 \frac{d}{d\theta} M(t+\theta)\Delta u(t+\theta)d\theta\| \leq \delta_2 \quad (15b)$$

$$\begin{aligned} \|\chi_3\| &= \|M^{-1}\{(\bar{M} - M)\ddot{q}^d + (M_L - \bar{M})\ddot{q}_L^d \\ &- \int_{-L}^0 \frac{d}{d\theta} H(t+\theta)d\theta\}\| \leq \delta_3 \end{aligned} \quad (15c)$$

$$\|\chi_4\| = \|(I - M^{-1}\bar{M})D\xi\| \leq \|ED\|\|\xi\| \quad (15d)$$

$$\begin{aligned} \|\chi_5\| &= \|M^{-1} \int_{-L}^0 \frac{d}{d\theta} (\bar{M} - M(t+\theta))D\xi(t+\theta)d\theta \\ &+ (I - M^{-1}\bar{M})D\xi\| \leq \|ED\|\|\xi\| + \delta_5 \end{aligned} \quad (15e)$$

$$\|\chi_6\| = \|E\sigma + M^{-1} \int_{-L}^0 \frac{d}{d\theta} \{(M(t+\theta) - \bar{M})\sigma(t+\theta)\}d\theta\| \leq \|E\|\|\sigma\| + \delta_6. \quad (15g)$$

Here M and H are explicitly represented in time for ease of notation. The upper bound of $\|\sigma\|$ is formulated

using (15a)-(15g) from (14) as

$$\|\sigma\| \leq \beta_0^* + \beta_1^* \|D\| \|\xi\|, \quad (16)$$

$$\text{where } \beta_0^* = \frac{\sum_{i=1}^6 \delta_i}{1 - \|E\|}, \quad \beta_1^* = \frac{2\|E\|}{1 - \|E\|}$$

under the following condition

$$\|E\| = \|I - M^{-1}\bar{M}\| < 1. \quad (17)$$

Remark 3 (Choice of \bar{M} and upper bound of $\|\sigma\|$): The condition (17) is standard in the TDE literature [7]–[10] and hence, the proposed formulation does not introduce any additional design condition. Further, from the upper bound on M (cf. Remark 1), one can always design \bar{M} to satisfy (17). It is noteworthy that the upper bound structure of $\|\sigma\|$, involving both states and their constraints, is unique compared to the existing literature ([1]–[13]), and thus requires a new adaptive control framework as derived subsequently.

B. Adaptive law design

The error dynamics (8) can be re-written in form of

$$\dot{\xi} = (A_0 + \bar{A})\xi + B(\sigma - \Delta u), \quad (18)$$

where $B = \begin{bmatrix} 0 \\ I_n \end{bmatrix}$, $A_0 = \begin{bmatrix} -\lambda_P & 0 \\ 0 & -\lambda_D \end{bmatrix}$, $\bar{A} = \begin{bmatrix} \lambda_P & I_n \\ -D_P & -D_D + \lambda_D \end{bmatrix}$ and $\lambda_P = \text{diag}\{\lambda_{p1}, \dots, \lambda_{pn}\}$, $\lambda_D = \text{diag}\{\lambda_{d1}, \dots, \lambda_{dn}\}$ are user-defined positive definite diagonal matrices with $\lambda_{pi}, \lambda_{di} \in \mathbb{R}^+$ for each $i = 1, 2, \dots, n$.

The term Δu is designed as

$$\Delta u(t) = \rho \frac{s}{\|s\|}, \quad (19)$$

where $s = B^T D_\xi \xi$ and $D_\xi = \text{diag}\{D_P, D_D\}$. The adaptive gain ρ in (19) is formulated based on the upper bound structure of $\|\sigma\|$ from (16) as

$$\rho = \hat{\beta}_0 + \hat{\beta}_1 \|D\| \|\xi\| + \zeta, \quad (20)$$

where $\hat{\beta}_0, \hat{\beta}_1$ are the estimates of $\beta_0, \beta_1 \in \mathbb{R}^+$, respectively and adapted via the following laws:

$$\dot{\hat{\beta}}_0 = \|s\| - \nu_0 \hat{\beta}_0, \quad \hat{\beta}_0(0) > 0, \quad (21a)$$

$$\dot{\hat{\beta}}_1 = \|s\| \|D\| \|\xi\| - \nu_1 \hat{\beta}_1, \quad \hat{\beta}_1(0) > 0, \quad (21b)$$

$$\dot{\zeta} = -(1 + \|D_\xi\| \|\bar{A}\| \|\xi\|^2) \zeta + \epsilon, \quad (21c)$$

$$- \sum_{i=1}^n \frac{\dot{k}_{pi}}{k_{pi}} \left[\frac{e_i^2}{k_{pi}^2 - e_i^2} \right] - \sum_{i=1}^n \frac{\dot{k}_{vi}}{k_{vi}} \left[\frac{\dot{e}_i^2}{k_{vi}^2 - \dot{e}_i^2} \right] \Big) \zeta + \epsilon,$$

where $\nu_i, \epsilon \in \mathbb{R}^+$ are user-defined scalars. Finally, combining (7a) and (19) becomes

$$\tau = \underbrace{\tau_L - \bar{M}\ddot{q}_L}_{\text{TDE part}} + \underbrace{\bar{M}(\ddot{q}^d + D_D \dot{e} + D_P e)}_{\text{Desired error constraint part}} + \underbrace{\rho s / \|s\|}_{\text{Adaptive part}}. \quad (22)$$

Remark 4 (Choice of L): The upper bounds in (15a)-(15g) reveal that high value of time delay L will lead to high values of δ_i , i.e., larger TDE error. Therefore, L is to be selected as the smallest possible sampling time of the low level micro-controller, which is consistent with traditional TDE-based literature [9], [10].

Remark 5: It may appear from (7d) that the gains D_P and D_D will become infeasible if the error variables touch the constraints. However, the subsequent closed-loop stability analysis will show that the tracking errors never violate the constraints with the proposed control design.

IV. CLOSED-LOOP SYSTEM STABILITY

Theorem 1: Under Property 1 and using the proposed control laws (22), along with the adaptive law (21) and the design condition (17), the tracking error trajectories e and \dot{e} remain within the bounds defined in (6) for all $t \geq 0$.

Proof: Modeling the adaptive laws (21a) as linear time-varying systems, and using their analytical solutions from positive initial conditions, it can be verified that $\hat{\beta}_0, \hat{\beta}_1 \geq 0$ and from (21c), it can be verified that $\exists \bar{\zeta}, \underline{\zeta} \in \mathbb{R}^+$ such that

$$0 < \underline{\zeta} \leq \zeta(t) \leq \bar{\zeta}, \quad \forall t > 0. \quad (23)$$

Stability is analyzed using the following Lyapunov function:

$$V = \frac{1}{2} \sum_{i=1}^n \log \left(\frac{k_{pi}^2}{k_{pi}^2 - e_i^2} \right) + \frac{1}{2} \sum_{i=1}^n \log \left(\frac{k_{vi}^2}{k_{vi}^2 - \dot{e}_i^2} \right) + \sum_{j=0}^1 \frac{(\hat{\beta}_j - \beta_j^*)^2}{2} + \frac{\zeta}{\underline{\zeta}}, \quad (24)$$

Taking the time derivative of (24)

$$\begin{aligned} \dot{V} &= \sum_{i=1}^n \left(\frac{e_i \dot{e}_i}{k_{pi}^2 - e_i^2} + \frac{\dot{k}_{pi}}{k_{pi}} - \frac{k_{pi} \dot{k}_{pi}}{k_{pi}^2 - e_i^2} \right) + \sum_{j=0}^1 (\hat{\beta}_j - \beta_j^*) \dot{\hat{\beta}}_j \\ &+ \sum_{i=1}^n \left(\frac{\dot{e}_i \ddot{e}_i}{k_{vi}^2 - \dot{e}_i^2} + \frac{\dot{k}_{vi}}{k_{vi}} - \frac{k_{vi} \dot{k}_{vi}}{k_{vi}^2 - \dot{e}_i^2} \right) + \frac{\dot{\zeta}}{\underline{\zeta}} \\ &= e^T D_P \dot{e} + \dot{e}^T D_D \ddot{e} + \sum_{j=0}^1 (\hat{\beta}_j - \beta_j^*) \dot{\hat{\beta}}_j + \frac{\dot{\zeta}}{\underline{\zeta}} \\ &+ \sum_{i=1}^n \left(\frac{\dot{k}_{vi}}{k_{vi}} - \frac{k_{vi} \dot{k}_{vi}}{k_{vi}^2 - \dot{e}_i^2} + \frac{\dot{k}_{pi}}{k_{pi}} - \frac{k_{pi} \dot{k}_{pi}}{k_{pi}^2 - e_i^2} \right) \\ &= \xi^T D_\xi \dot{\xi} + \sum_{j=0}^1 (\hat{\beta}_j - \beta_j^*) \dot{\hat{\beta}}_j + \frac{\dot{\zeta}}{\underline{\zeta}} \\ &+ \sum_{i=1}^n \left(\frac{\dot{k}_{vi}}{k_{vi}} - \frac{k_{vi} \dot{k}_{vi}}{k_{vi}^2 - \dot{e}_i^2} + \frac{\dot{k}_{pi}}{k_{pi}} - \frac{k_{pi} \dot{k}_{pi}}{k_{pi}^2 - e_i^2} \right). \quad (25) \end{aligned}$$

Using (18) one can get

$$\begin{aligned}
\dot{V} &= \xi^T D_\xi A_0 \xi + \xi^T D_\xi \bar{A} \xi + \xi^T D_\xi B (\sigma - \Delta u) + \frac{\dot{\zeta}}{\zeta} \\
&+ \sum_{i=1}^n \left(\frac{\dot{k}_{vi}}{k_{vi}} - \frac{k_{vi} \dot{k}_{vi}}{k_{vi}^2 - e_i^2} + \frac{\dot{k}_{pi}}{k_{pi}} - \frac{k_{pi} \dot{k}_{pi}}{k_{pi}^2 - e_i^2} \right) + \sum_{j=0}^1 (\hat{\beta}_j - \beta_j^*) \dot{\hat{\beta}}_j \\
&\leq \xi^T D_\xi A_0 \xi + \|D_\xi\| \|\bar{A}\| \|\xi\|^2 + \|s\| \|\sigma\| - \rho \|s\| + \frac{\dot{\zeta}}{\zeta} \\
&+ \sum_{i=1}^n \left(\frac{\dot{k}_{vi}}{k_{vi}} - \frac{k_{vi} \dot{k}_{vi}}{k_{vi}^2 - e_i^2} + \frac{\dot{k}_{pi}}{k_{pi}} - \frac{k_{pi} \dot{k}_{pi}}{k_{pi}^2 - e_i^2} \right) + \sum_{j=0}^1 (\hat{\beta}_j - \beta_j^*) \dot{\hat{\beta}}_j \\
&\leq \xi^T D_\xi A_0 \xi + \|D_\xi\| \|\bar{A}\| \|\xi\|^2 - (\hat{\beta}_0 - \beta_0^*) \|s\| \\
&- (\hat{\beta}_1 - \beta_1^*) (\|s\| \|\xi\| \|D\|) + \sum_{j=0}^1 (\hat{\beta}_j - \beta_j^*) \dot{\hat{\beta}}_j + \frac{\dot{\zeta}}{\zeta} \\
&+ \sum_{i=1}^n \left(\frac{\dot{k}_{vi}}{k_{vi}} - \frac{k_{vi} \dot{k}_{vi}}{k_{vi}^2 - e_i^2} + \frac{\dot{k}_{pi}}{k_{pi}} - \frac{k_{pi} \dot{k}_{pi}}{k_{pi}^2 - e_i^2} \right). \quad (26)
\end{aligned}$$

Also, from (21a) we have

$$\begin{aligned}
\sum_{j=0}^1 (\hat{\beta}_j - \beta_j^*) \dot{\hat{\beta}}_j &= (\hat{\beta}_0 - \beta_0^*) (\|s\| - \nu_0 \hat{\beta}_0) \\
&+ (\hat{\beta}_1 - \beta_1^*) (\|s\| \|\xi\| \|D\| - \nu_1 \hat{\beta}_1) \\
&= (\hat{\beta}_0 - \beta_0^*) \|s\| + (\hat{\beta}_1 - \beta_1^*) (\|s\| \|\xi\| \|D\|) \\
&+ \sum_{j=0}^1 (\nu_j \hat{\beta}_j \beta_j^* - \nu_j \hat{\beta}_j^2). \quad (27)
\end{aligned}$$

One can verify that

$$(\nu_j \hat{\beta}_j \beta_j^* - \nu_j \hat{\beta}_j^2) = -\frac{\nu_j}{2} \left((\hat{\beta}_j - \beta_j^*)^2 - \beta_j^{*2} \right). \quad (28)$$

For $l = p, v$ and $\mu = e, \dot{e}$, we can simplify

$$\sum_{i=1}^n \frac{\dot{k}_{li}}{k_{li}} - \frac{k_{li} \dot{k}_{li}}{k_{li}^2 - \mu_i^2} = -\sum_{i=1}^n \frac{\dot{k}_{li}}{k_{li}} \left[\frac{\mu_i^2}{k_{li}^2 - \mu_i^2} \right] \quad (29)$$

The adaptive law (21c) and relation (23) lead to

$$\begin{aligned}
\frac{\dot{\zeta}}{\zeta} &\leq -\|D_\xi\| \|\bar{A}\| \|\xi\|^2 + \sum_{i=1}^n \frac{\dot{k}_{pi}}{k_{pi}} \left[\frac{e_i^2}{k_{pi}^2 - e_i^2} \right] \\
&+ \sum_{i=1}^n \frac{\dot{k}_{vi}}{k_{vi}} \left[\frac{e_i^2}{k_{vi}^2 - e_i^2} \right] + \frac{\epsilon}{\zeta}. \quad (30)
\end{aligned}$$

Using results from (27),(28),(29),(30) into (26), give

$$\begin{aligned}
\dot{V} &= \xi^T D_\xi A_0 \xi - \sum_{j=0}^1 \frac{\nu_j}{2} \left((\hat{\beta}_j - \beta_j^*)^2 - \beta_j^{*2} \right) + \frac{\epsilon}{\zeta} \\
&= -[e^T \quad \dot{e}^T] \begin{bmatrix} D_p \lambda_p & 0 \\ 0 & D_d \lambda_d \end{bmatrix} \begin{bmatrix} e \\ \dot{e} \end{bmatrix} \\
&- \sum_{j=0}^1 \frac{\nu_j}{2} \left((\hat{\beta}_j - \beta_j^*)^2 - \beta_j^{*2} \right) + \frac{\epsilon}{\zeta} \\
&= -\sum_{i=1}^n \lambda_{pi} \left(\frac{e_i^2}{k_{pi}^2 - e_i^2} \right) - \sum_{i=1}^n \lambda_{di} \left(\frac{e_i^2}{k_{vi}^2 - e_i^2} \right) \\
&- \sum_{j=0}^1 \frac{\nu_j}{2} \left((\hat{\beta}_j - \beta_j^*)^2 - \beta_j^{*2} \right) + \frac{\epsilon}{\zeta}. \quad (31)
\end{aligned}$$

From the fact that $\log\left(\frac{k_x^2}{k_x^2 - x^2}\right) < \frac{x^2}{k_x^2 - x^2}$, for $|x| < k_x$, which holds within any compact set $\Omega : |x| < k_x$, and for any $k_x \in \mathbb{R}_+$, we can write

$$\begin{aligned}
\dot{V} &\leq -\sum_{i=1}^n \lambda_{pi} \log\left(\frac{k_{pi}^2}{k_{pi}^2 - e_i^2}\right) - \sum_{i=1}^n \lambda_{di} \log\left(\frac{k_{vi}^2}{k_{vi}^2 - e_i^2}\right) \\
&- \sum_{j=0}^1 \frac{\nu_j}{2} \left((\hat{\beta}_j - \beta_j^*)^2 - \beta_j^{*2} \right) + \frac{\epsilon}{\zeta}. \quad (32)
\end{aligned}$$

The definition of V as in (24) yields

$$\begin{aligned}
V &= \frac{1}{2} \sum_{i=1}^n \log\left(\frac{k_{pi}^2}{k_{pi}^2 - e_i^2}\right) + \frac{1}{2} \sum_{i=1}^n \log\left(\frac{k_{vi}^2}{k_{vi}^2 - e_i^2}\right) \\
&+ \sum_{j=0}^1 \frac{(\hat{\beta}_j - \beta_j^*)^2}{2} + \frac{\bar{\zeta}}{\zeta}. \quad (33)
\end{aligned}$$

Combining \dot{V} and V from (32) and (33)

$$\dot{V} \leq -\varrho V + \varrho \frac{\bar{\zeta}}{\zeta} + \frac{\epsilon}{\zeta} + \frac{1}{2} \sum_{i=0}^1 \nu_i \beta_i^{*2} \quad (34)$$

where $\varrho \triangleq \min\{\min\{\lambda_{pi}\}, \min\{\lambda_{di}\}, \nu_{pi}/2\}$. ■

Remark 6 (Continuity in control law): To make the control laws continuous for practical implementation, the terms $(s/\|s\|)$ are usually replaced by continuous saturation functions $\text{sat}(s, \varpi)$ for $\varpi \in \mathbb{R}^+$ (cf. the notation definition in Sect. I): this still keeps the closed-loop system bounded with minor modification in stability analysis (cf. [39]), and hence repetition is avoided.

Algorithm 1 Design steps of the proposed controller

Step 1 (Selection of the constraints): Select the values of various parameters of the time-varying constraints, i.e., of the steady-state bounds (k_{sspi}, k_{ssvi}) , of the initial values (k_{0pi}, k_{0vi}) , and of the parameters $(\alpha_{pi}, \alpha_{vi})$ as per requirements, following Remark 2.

Step 2 (Defining control gains): Define state-constraint gains D_P and D_D based upon the parameters selected in Step 1.

Step 3 (Designing adaptive controller): Define s , gains λ_P, λ_D and ρ as in (20) using adaptive laws in (21).

Step 4 (Defining control input): Select \bar{M} using (17) and use the values chosen in Steps 1-3 to design the control inputs τ as given in (22).

V. EXPERIMENTAL VALIDATION AND RESULTS

The experimental platform consisted of UFactory 5-DoF xArm-5 robotic manipulator (cf. Fig. 1), with an NVIDIA Jetson AGX Xavier serving as the compute unit. A custom-designed end-effector was attached, incorporating a Dynamixel XM430-W210-T servo motor to enable rapid switching between two tools: a marker and an eraser. This configuration allows for seamless

tool transitions during task execution. Real-time joint state data were acquired via the manipulator’s internal feedback interface, supporting synchronized, high-frequency closed-loop control.

A. Experimental Scenario

The robot was commanded to perform a constrained drawing and erasing task on a surface: drawing of 3 layers of concentric semicircles and then erase the middle semicircle without erasing/ disturbing the inner and outer semicircles. Involving physical contact and tight position and velocity limits in the task was designed to evaluate tracking performance and constraint handling under state-dependent and external disturbances arising from unknown surface contact forces and frictional variations at the end-effector. The specific sequences of the task are as follows:

- Starting from the initial position, draw an innermost semicircle with a radius of 20 cm; lift the pen and come back to the initial position.
- Draw an outermost semicircle with a radius of 24 cm; lift the pen and come back to the initial position.
- Draw a middle semicircle with a radius of 22 cm; lift the pen and come back to the initial position.
- Rotate the tool (from drawing to erasing) and erase the middle (22 cm) semicircle using the eraser starting from the initial position.

Both the drawing and erasing of the middle semicircle occur in a confined region between the inner and outer paths, thereby emphasizing the critical role of real-time constraint enforcement to ensure safe and feasible motion. The desired trajectory (q^d, \dot{q}^d) for the manipulator is pre-computed using the open-source package named *ruckig* [40]. The 4 cm radial distance between the inner and outer semicircles was selected to accommodate the 2 cm wide eraser. It is important to note that the initial condition of the robot is always set at zero (as provided by the manufacturer). Therefore, the initial error always starts from zero (cf. the experimental error plots later).

To evaluate the significance of the proposed control strategy, its performance was compared against two representative baselines: (i) an adaptive BLF-based controller [32] (referred as ABLF) and (ii) an adaptive TDE-based controller [11] (referred ATDC). The parameters used in the experiments for the proposed controller are listed in Table I along with parameters to design the constraints. For both baselines, the controller gains were carefully tuned according to the respective design guidance to achieve their best possible performance under identical task conditions.

B. Results and Analysis

The performance of the controllers is illustrated in Figs. 2–4. Figure 2 clearly illustrates that the semicir-

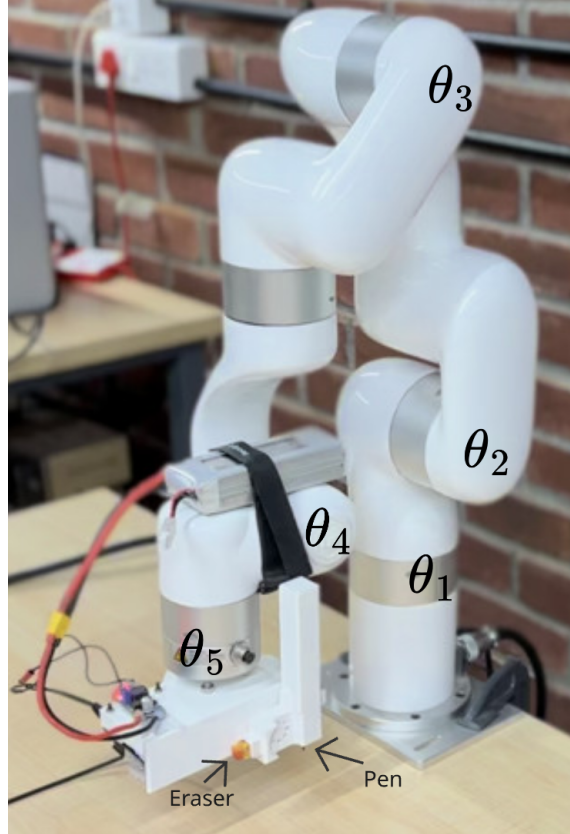


Fig. 1. Experimental setup of 5-DoF xArm and custom end-effector.

TABLE I
DESIGN PARAMETERS FOR THE PROPOSED CONTROLLER

$\bar{M} = I; \lambda_D = \text{diag}\{3, 3, 3, 3, 3\}; \lambda_P = \text{diag}\{5, 5, 5, 5, 5\}$ $L = 0.01$ $\hat{\beta}_0(0) = \hat{\beta}_1(0) = 0.01; \nu_0 = \nu_1 = 10.0$ $\zeta(0) = 0.1; \epsilon = 0.0001$ $k_{0p1} = k_{0p2} = k_{0p3} = k_{0p4} = k_{0p5} = 10.0$ $k_{0v1} = k_{0v2} = k_{0v3} = k_{0v4} = k_{0v5} = 20.0$ $k_{ssp1} = k_{ssp2} = k_{ssp3} = k_{ssp4} = k_{ssp5} = 5.0$ $k_{ssv1} = k_{ssv2} = k_{ssv3} = k_{ssv4} = k_{ssv5} = 10.0$ $\alpha_p = \alpha_v = 0.075$
--

cles drawn by the proposed controller closely match the intended trajectories, while those produced by the baseline controllers exhibit noticeable distortions. The results clearly demonstrate that the proposed controller outperforms the baselines in both tracking accuracy and constraint satisfaction. As shown in the tracking error plots 3–4, it consistently keeps the tracking errors within the prescribed position and velocity bounds—a direct result of its integrated adaptive time-delay estimation and BLF-based constraint handling.

These qualitative trends are further substantiated by the quantitative results in Table II, where the proposed controller achieves the lowest Root Mean Square (RMS)

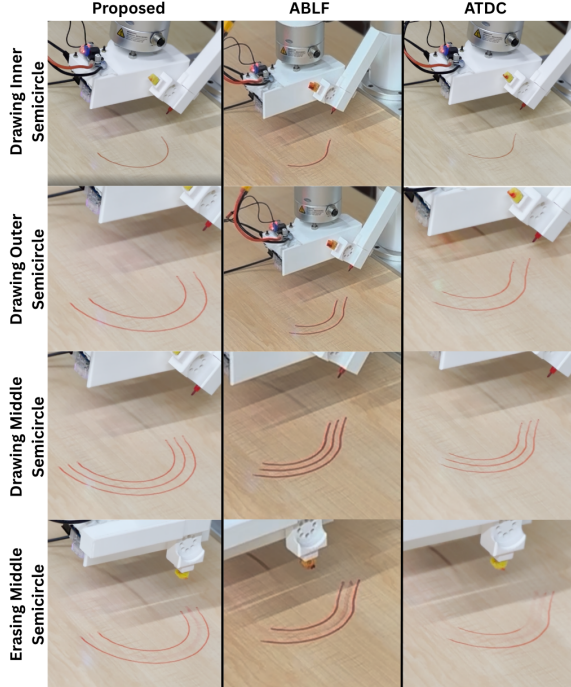


Fig. 2. Controller comparison during the constrained drawing-erasing task. Columns: Proposed, ABLF, and ATDC. Rows: drawing inner semicircle, drawing outer semicircle, drawing middle semicircle, and erasing the middle semicircle.

TABLE II
PERFORMANCE COMPARISON IN RMS ERROR

		θ_1	θ_2	θ_3	θ_4	θ_5
Position error (deg)	Proposed	0.64	1.06	0.82	0.98	0.63
	ABLF	1.06	1.75	1.41	1.63	1.04
	ATDC	2.31	4.04	3.63	3.91	2.30
Velocity error (deg/s)	Proposed	2.40	2.19	3.10	2.24	1.79
	ABLF	3.88	4.26	3.82	4.12	3.87
	ATDC	4.06	6.72	6.31	7.32	4.01

errors across all joints. ABLF, equipped with constraint handling capability, could honor the constraints; however, it cannot negotiate state-dependent and unmodelled uncertainties, leading to distorted drawings. Although ATDC can tackle state-dependent uncertainty, it lacks the ability to handle constraint; consequently, ATDC partially erases the inner and outer semicircles, which is unintended. These observations highlight that the capability to handle either the state-dependent uncertainty or the state constraints alone is not sufficient; a control framework, like the proposed one, must combine both these features to achieve the desired result.

VI. CONCLUSIONS

This paper presented a unified adaptive-robust control framework that integrates time-delay estimation with BLF-based constraint enforcement for Euler-Lagrange robotic systems under state-dependent uncertainties. The

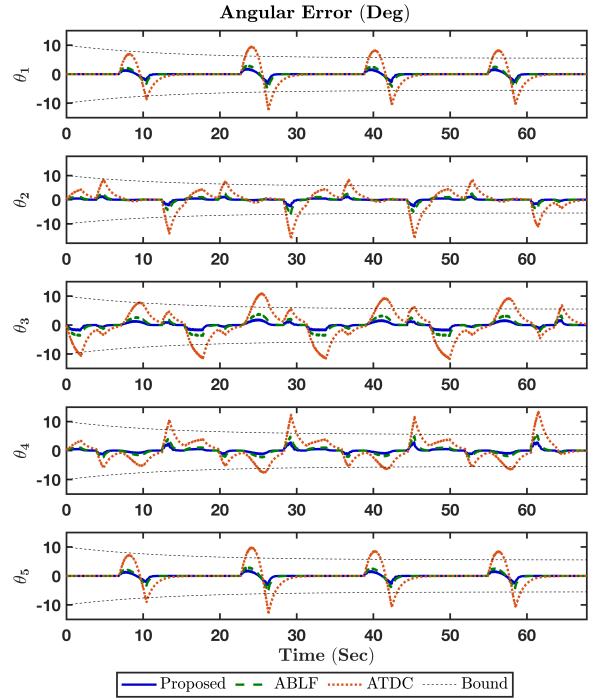


Fig. 3. Joint angle tracking error performance comparison.

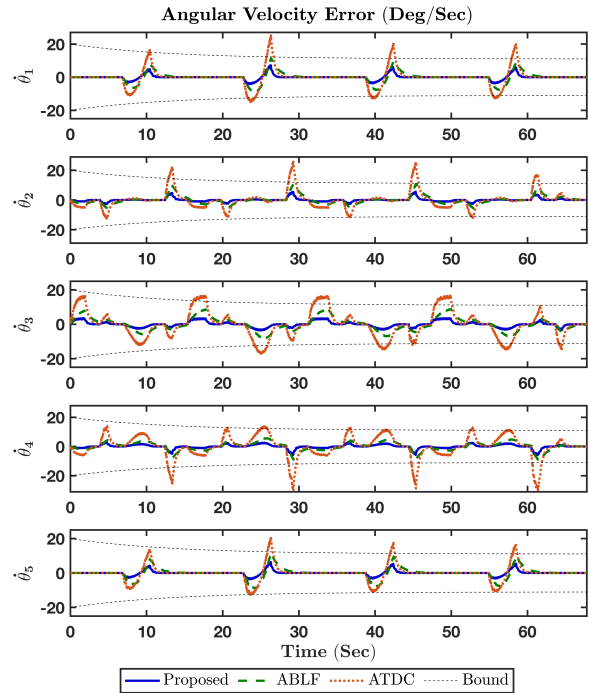


Fig. 4. Joint velocity tracking errors performance comparison.

proposed approach achieves real-time tracking while rigorously satisfying time-varying position and velocity constraints—without requiring prior model knowledge. Experimental validation on a 5-DoF robotic manipulator demonstrated the superior performance of the proposed controller over the state-of-the-art in contact-rich tasks, achieving lower tracking errors and strict constraint compliance. A future work would be to extend the proposed framework for underactuated robotic systems.

REFERENCES

- [1] T. Hsia, T. Lasky, and Z. Guo, “Robust independent joint controller design for industrial robot manipulators,” *IEEE Trans. Ind. Electron.*, vol. 38, no. 1, pp. 21–25, 1991.
- [2] K. Youcef-Toumi and O. Ito, “A time delay controller for systems with unknown dynamics,” in *1988 American Control Conference*, 1988, pp. 904–913.
- [3] J. Kim, H. Joe, S.-c. Yu, J. S. Lee, and M. Kim, “Time-delay controller design for position control of autonomous underwater vehicle under disturbances,” *IEEE Trans. Ind. Electron.*, vol. 63, no. 2, pp. 1052–1061, 2016.
- [4] M. Jin, J. Lee, and N. G. Tsagarakis, “Model-free robust adaptive control of humanoid robots with flexible joints,” *IEEE Trans. Ind. Electron.*, vol. 64, no. 2, pp. 1706–1715, 2017.
- [5] M. Jin, J. Lee, P. H. Chang, and C. Choi, “Practical nonsingular terminal sliding-mode control of robot manipulators for high-accuracy tracking control,” *IEEE Trans. Ind. Electron.*, vol. 56, no. 9, pp. 3593–3601, 2009.
- [6] M. Jin, S. H. Kang, and P. H. Chang, “Robust compliant motion control of robot with nonlinear friction using time-delay estimation,” *IEEE Trans. Ind. Electron.*, vol. 55, no. 1, pp. 258–269, 2008.
- [7] S. Roy, I. N. Kar, J. Lee, N. G. Tsagarakis, and D. G. Caldwell, “Adaptive-robust control of a class of EL systems with parametric variations using artificially delayed input and position feedback,” *IEEE Trans. Control Syst. Technol.*, vol. 27, no. 2, pp. 603–615, 2019.
- [8] M. Pi, Y. Kang, C. Xu, G. Li, and Z. Li, “Adaptive time-delay balance control of biped robots,” *IEEE Trans. Ind. Electron.*, vol. 67, no. 4, pp. 2936–2944, 2020.
- [9] D. D. Dhadekar, P. D. Sanghani, K. Mangrulkar, and S. Talole, “Robust control of quadrotor using uncertainty and disturbance estimation,” *Journal of Intelligent & Robotic Systems*, vol. 101, pp. 1–21, 2021.
- [10] B. Lim, J. Jang, J. Lee, B. Choi, Y. Lee, and Y. Shim, “Delayed output feedback control for gait assistance and resistance using a robotic exoskeleton,” *IEEE Rob. Autom. Lett.*, vol. 4, no. 4, pp. 3521–3528, 2019.
- [11] S. Roy, J. Lee, and S. Baldi, “A new adaptive-robust design for time delay control under state-dependent stability condition,” *IEEE Trans. Control Syst. Technol.*, vol. 29, no. 1, pp. 420–427, 2021.
- [12] S. Dantu, R. D. Yadav, S. Roy, J. Lee, and S. Baldi, “Adaptive artificial time delay control for quadrotors under state-dependent unknown dynamics,” in *2022 IEEE International Conference on Robotics and Biomimetics (ROBIO)*, 2022, pp. 1092–1097.
- [13] S. Roy, S. Baldi, P. Li, and V. N. Sankaranarayanan, “Artificial-delay adaptive control for underactuated Euler–Lagrange robotics,” *IEEE/ASME Trans. Mechatron.*, vol. 26, no. 6, pp. 3064–3075, 2021.
- [14] A. Dhar and S. Bhasin, “Indirect adaptive MPC for discrete-time LTI systems with parametric uncertainties,” *IEEE Trans. Autom. Control*, vol. 66, no. 11, pp. 5498–5505, 2021.
- [15] J. Berberich, J. Köhler, M. A. Müller, and F. Allgöwer, “Data-driven model predictive control with stability and robustness guarantees,” *IEEE Trans. Autom. Control*, vol. 66, no. 4, pp. 1702–1717, 2020.
- [16] L. Grüne, J. Pannek, and L. Grüne, *Nonlinear Model Predictive Control*. Springer, 2017.
- [17] R. Tao, P. Zhao, I. Kolmanovsky, and N. Hovakimyan, “Robust adaptive MPC using uncertainty compensation,” in *2024 American Control Conference (ACC)*, 2024, pp. 1873–1878.
- [18] K. P. Tee, S. S. Ge, and E. H. Tay, “Barrier Lyapunov functions for the control of output-constrained nonlinear systems,” *Automatica*, vol. 45, no. 4, pp. 918–927, 2009.
- [19] Y.-J. Liu and S. Tong, “Barrier Lyapunov functions-based adaptive control for a class of nonlinear pure-feedback systems with full state constraints,” *Automatica*, vol. 64, pp. 70–75, 2016.
- [20] Y. Cao, J. Cao, and Y. Song, “Practical prescribed time tracking control over infinite time interval involving mismatched uncertainties and non-vanishing disturbances,” *Automatica*, vol. 136, p. 110050, 2022.
- [21] V. N. Sankaranarayanan, R. D. Yadav, R. K. Swayampakula, S. Ganguly, and S. Roy, “Robustifying payload carrying operations for quadrotors under time-varying state constraints and uncertainty,” *IEEE Rob. Autom. Lett.*, vol. 7, no. 2, pp. 4885–4892, 2022.
- [22] S. Ganguly, V. N. Sankaranarayanan, B. Suraj, R. D. Yadav, and S. Roy, “Robust manoeuvring of quadrotor under full state constraints,” *IFAC-PapersOnLine*, vol. 55, no. 1, pp. 32–37, 2022.
- [23] S. Ganguly, V. N. Sankaranarayanan, B. V. S. G. Suraj, R. Dev Yadav, and S. Roy, “Efficient manoeuvring of quadrotor under constrained space and predefined accuracy,” in *2021 IEEE/RSJ International Conference on Intelligent Robots and Systems (IROS)*, 2021, pp. 6352–6357.
- [24] F. Xu, L. Tang, and Y.-J. Liu, “Tangent barrier Lyapunov function-based constrained control of flexible manipulator system with actuator failure,” *International Journal of Robust and Nonlinear Control*, vol. 31, no. 17, pp. 8523–8536, 2021.
- [25] D. Cruz-Ortiz, I. Chairez, and A. Poznyak, “Non-singular terminal sliding-mode control for a manipulator robot using a barrier Lyapunov function,” *ISA Transactions*, vol. 121, pp. 268–283, 2022.
- [26] Y.-J. Liu and S. Tong, “Barrier Lyapunov functions for nussbaum gain adaptive control of full state constrained nonlinear systems,” *Automatica*, vol. 76, pp. 143–152, 2017.
- [27] K. Shao, R. Tang, F. Xu, X. Wang, and J. Zheng, “Adaptive sliding mode control for uncertain Euler–Lagrange systems with input saturation,” *J. Franklin Inst.*, vol. 358, no. 16, pp. 8356–8376, 2021.
- [28] H. Pang, X. Zhang, and Z. Xu, “Adaptive backstepping-based tracking control design for nonlinear active suspension system with parameter uncertainties and safety constraints,” *ISA Transactions*, vol. 88, pp. 23–36, 2019.
- [29] D. Yang, X. Gao, E. Cui, and Z. Ma, “State-constraints adaptive backstepping control for active magnetic bearings with parameters nonstationarities and uncertainties,” *IEEE Trans. Ind. Electron.*, vol. 68, no. 10, pp. 9822–9831, 2020.
- [30] H. Obeid, L. M. Fridman, S. Laghrouche, and M. Harmouche, “Barrier function-based adaptive sliding mode control,” *Automatica*, vol. 93, pp. 540–544, 2018.
- [31] S. Laghrouche, M. Harmouche, Y. Chitour, H. Obeid, and L. M. Fridman, “Barrier function-based adaptive higher order sliding mode controllers,” *Automatica*, vol. 123, p. 109355, 2021.
- [32] C. Liu, X. Liu, H. Wang, Y. Zhou, and S. Lu, “Finite-time adaptive tracking control for unknown nonlinear systems with a novel barrier Lyapunov function,” *Inf. Sci.*, vol. 528, pp. 231–245, 2020.
- [33] S. Ding, B. Zhang, K. Mei, and J. H. Park, “Adaptive fuzzy SOSM controller design with output constraints,” *IEEE Trans. Fuzzy Syst.*, vol. 30, no. 7, pp. 2300–2311, 2021.
- [34] Y.-J. Liu, L. Ma, L. Liu, S. Tong, and C. P. Chen, “Adaptive neural network learning controller design for a class of nonlinear systems with time-varying state constraints,” *IEEE Trans. Neural Networks Learn. Syst.*, vol. 31, no. 1, pp. 66–75, 2019.
- [35] R. Q. Fuentes-Aguilar and I. Chairez, “Adaptive tracking control of state constraint systems based on differential neural networks:

- A barrier Lyapunov function approach,” *IEEE Trans. Neural Networks Learn. Syst.*, vol. 31, no. 12, pp. 5390–5401, 2020.
- [36] S. Roy and S. Baldi, “Towards structure-independent stabilization for uncertain underactuated Euler–Lagrange systems,” *Automatica*, vol. 113, p. 108775, 2020.
- [37] M. W. Spong, S. Hutchinson, and M. Vidyasagar, *Robot modeling and control*. Wiley New York, 2006, vol. 3.
- [38] W. Rudin, “Principles of mathematical analysis,” 3rd ed., 1976.
- [39] S. Roy, S. B. Roy, J. Lee, and S. Baldi, “Overcoming the underestimation and overestimation problems in adaptive sliding mode control,” *IEEE/ASME Trans. Mechatron.*, vol. 24, no. 5, pp. 2031–2039, 2019.
- [40] L. Berscheid and T. Kröger, “Jerk-limited real-time trajectory generation with arbitrary target states,” *Robotics: Science and Systems XVII*, 2021.